Journal of Casting & Materials Engineering Vol. 9 No. 4 (2025) 72–79
https://doi.org/10.7494/jcme.2025.9.4.72

Reverse Engineering and Computer Modelling in Archaeometallurgy for the Reconstruction of Heritage Objects Using Precision Casting and 3D Printing

Karolina Marlicka[a,*], Andrzej Fijołek[a], Aldona Garbacz-Klempka[a], Marcin Piękoś[a]

[a]AGH University of Krakow, Faculty of Foundry Engineering, 23 Reymonta St., 30 059 Krakow, Poland
**e-mail: marlicka@agh.edu.pl*

Received: 21 November 2025/Accepted: 17 December 2025/Published online: 23 December 2025.
This article is published with open access at AGH University of Science and Technology Journals

Abstract

This article presents an interdisciplinary approach to the reconstruction of a copper-alloy artefact using reverse engineering techniques combined with modern digital and manufacturing technologies. The research was motivated by the need to better understand historical casting techniques while preserving the integrity of cultural heritage objects through non-destructive methods. The study integrates 3D scanning, CAD-based modelling, numerical simulations, investment casting, and metal additive manufacturing.

The geometry of the artefact was captured using high-resolution 3D scanning, enabling the development of two CAD models: one representing the preserved state of the object and a second reconstructed model with the missing fragment digitally restored. Both models were used for numerical simulations of mould filling, solidification, cooling, and porosity formation performed in MAGMASOFT® 6.1, allowing the assessment of technological feasibility and defect formation. Based on the simulation results, physical replicas were produced using investment casting and selective laser melting.

The obtained numerical and experimental results were compared in terms of geometry reproduction, surface characteristics, and predicted versus observed casting behaviour. The study demonstrates that the combination of digital reconstruction, simulation tools, and experimental manufacturing provides a reliable framework for analysing historical metallurgical processes. The proposed methodology supports both scientific interpretation and the practical reconstruction of heritage objects and can be applied to a wide range of archaeometallurgical studies.

Keywords:

casting, additive manufacturing technologies, 3D scan, computer modelling, numerical simulations, copper alloys, bronze, selective laser melting, investment casting, cultural heritage, archaeometallurgy, reconstruction

1. INTRODUCTION

The reconstruction of historical metallurgical techniques requires the simultaneous consideration of material properties, geometry, and the processes associated with casting. Small metal objects preserve within their structure information relating to the mould, the dynamics of metal flow, and the technical conditions that accompanied their production. Contemporary research approaches rely on non-destructive analyses, 3D scanning, computer modelling, and numerical simulations, complemented by experimental casting and additive manufacturing technologies [1–7].

In this article, research on a single artefact made of a copper alloy is presented. The chemical composition of this type of alloy is characteristic of castings produced during the period from which the analysed object originates and falls within the range typical of historical foundry materials. Surface analysis revealed the presence of material loss and preserved corrosion products, which served as the basis for the development of a 3D model and a geometric reconstruction. These models were used to conduct numerical simulations of the filling and solidification processes, casting, and 3D printing, enabling a comprehensive comparison of various reconstruction pathways [5–8].

2. MATERIALS AND METHODS

The study was carried out using non-destructive methods, 3D scanning with CAD modelling, and modern casting and additive manufacturing processes. In the first stage, three-dimensional documentation of the artefact was performed using the Revopoint POP2 3D scanner, whose detailed technical specification is presented in Table 1. The scanning was conducted with the use of a rotary table, which enabled the acquisition of a high-density point cloud. The obtained data were processed in the Revo Scan 5 software, where the scan was cleaned, the fragments were aligned, and a triangular mesh was generated. Final, the 3D geometry of the examined casting was obtained [9].

Table 1
Specification of the Revopoint POP2 scanner (technical documentation provided by Revopoint)

Technology	Dual camera infrared light
Single-frame precision	Up to 0.05 mm
Single-frame accuracy	Up to 0.1 mm
Single capture range	210 mm × 130 mm
Working distance	150–400 mm
Minimum scan volume	20 mm × 20 mm × 20 mm
Scanning speed	Up to 10 fps
Light source	Class 1 infrared light
Alignment	Feature, marker
Point distance/resolution	0.15 mm

Based on the 3D scans, two models were developed in the SOLIDWORKS 2023 environment: a real model, reflecting the preserved state, and a reconstructed model, in which the missing fragment was supplemented. These models were used both for numerical simulations and for 3D printing. The 3D modelling included an analysis of wall thickness, reconstruction of the missing structure, and preparation of solid bodies consistent with the requirements of casting simulation software and the metal 3D printer.

Three-dimensional scanning enabled the reconstruction of the overall geometry of the object, including its characteristic proportions and approximate dimensions. To better illustrate the scale of the analysed artefact, a schematic drawing presenting the general dimensions of the object was prepared (Fig. 1).

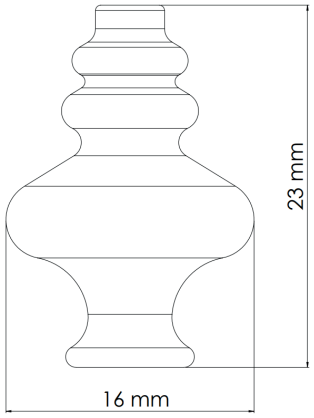

Fig. 1. Schematic drawing showing the approximate overall dimensions of the analysed object, prepared in SOLIDWORKS 2023

Numerical simulations of the mould filling, solidification, cooling, and porosity formation were carried out using the MAGMASOFT® 6.1 software. The simulations were based on previously prepared CAD models. For each model, appropriate functional roles were assigned within the simulation environment, and a virtual mould was generated, automatically adapting to the geometry of the casting.

The pouring parameters were defined individually for each object based on prior analyses. In the case of reconstructed forms, a CuSn12 alloy was applied, corresponding to one of the most commonly used bronze alloys in the Bronze Age. The pouring temperature was set to 1100°C in all simulations, ensuring optimal filling conditions for copper alloys. The pouring time was controlled by setting the filling level of the pouring basin to 70%, which enabled a stable metal flow and better reflected real casting conditions. The simulation results included temperature distribution after mould filling and predicted porosity distribution [2, 5].

The model intended for investment casting was exported to STL format and processed in CHITUBOX Basic V2.3, where the support system and model orientation were prepared. The replica was produced on an Elegoo Mars 3 3D printer using SuperCast-SuperFast (ENGR-A17L) photopolymer casting resin, designed for burnout processes in the investment casting technique. After completing the 3D printing, supports were removed and the model was cleaned, preparing it for moulding.

The mould was made using WiroFine refractory material, prepared in an AMX-1 vacuum mixer, which enabled thorough deaeration of the mass and ensured uniform consistency. The model was placed in metal cylinders, then filled with the refractory mass and left to solidify. The burnout and resin removal were carried out in an APE800 furnace in accordance with a predetermined temperature schedule: the mould was placed in a furnace preheated to 700°C, and the temperature was then increased by 50°C every 10 minutes, until reaching 1010°C, at which it was held for 60 minutes. This process enabled the complete burnout of the resin and the hardening of the ceramic shell [10, 11].

The casting was produced using the centrifugal method with a Pro-Dent WR02 casting centrifuge, which ensured the uniform filling of the mould with molten metal. The applied alloy was heated and melted in accordance with the technological parameters appropriate for this alloy system. After solidification, the ceramic mould was broken, and the casting was mechanically cleaned.

In parallel, a second technological replica was produced using metal 3D printing. The 3D model prepared in SOLIDWORKS 2023 was converted into a format compatible with a powder-bed printer and manufactured using the AL3D metal laser-sintering printer, employing the selective laser melting (SLM) method. The specification of the printer and the metal powder is also presented in Table 2. The additively manufactured reconstruction served to compare dimensional accuracy, surface characteristics, and potential differences resulting from alternative methods of producing low-mass objects with complex geometry [12–21].

Table 2
Specification of the AL3D printer (technical documentation provided by ALPHA LASER)

Process parameters	Open access to all machine and process parameters
Laser type	Fiber laser
Laser wave length	1,070 nm
Laser focal spot	0.05 mm
Laser scanning speed	Max. 5 m/s
Materials	m4p Brz10
Achievable component density	Up to 99%
Layer thickness	0.03 mm

The entire research procedure enabled the comparison of the geometry of the original object, the digital reconstruction, and the replicas produced using two different techniques, forming the basis for the further comparative analyses presented in subsequent chapters.

3. RESULTS

Surface observations revealed a visible metal loss with an irregular edge, as well as a depression covered with a greenish patina, which was left intact to preserve the structural integrity. The remaining surface areas showed features typical of small castings produced in moulds with characteristic micro-roughness.

3D scanning enabled precise reconstruction of the geometry, including variations in wall thickness in the damaged area. Figure 2 presents the CAD model of the preserved geometry, along with a magnification of the thinnest section. Figure 3 shows the reconstructed model, also with an enlarged view of the corresponding section, allowing for a direct comparison between the preserved state and the reconstruction.

Fig. 2. Model based on 3D scans developed in SOLIDWORKS 2023, with a close-up of a thin-walled section

Fig. 3. Reconstructed model developed in SOLIDWORKS 2023, with a close-up of a thin-walled section and the object's geometry reproduced

The transfer of both models into the MAGMASOFT® 6.1 software made it possible to perform numerical simulations. The filling of the scanned model, presented in Figure 4, proceeded smoothly, and the temperature distribution of the metal remained uniform. In subsequent stages of the filling process, no rapid temperature variations or indicating disturbances in the filling process were observed.

The solidification process of the scanned 3D model is shown in Figure 5. The temperature distribution progressed uniformly toward the gating system.

Analogous simulations were conducted for the reconstructed 3D model created in CAD software, where the filling behaviour shown in Figure 6, demonstrated nearly identical alloy behaviour compared to the scanned model. The solidification process, presented in Figure 7, progressed in accordance with the predicted pattern and remained consistent with the behaviour observed for the scanned model.

A comparative porosity analysis, the results of which are shown in Figure 8, indicated the presence of small porosity zones located in areas with characteristic geometric constrictions. In both models, a similar distribution of potential defects was predicted, resulting from local differences in solidification rates. At the same time, no concentrations of porosity were observed that could pose a significant threat to the structural integrity of the object during use.

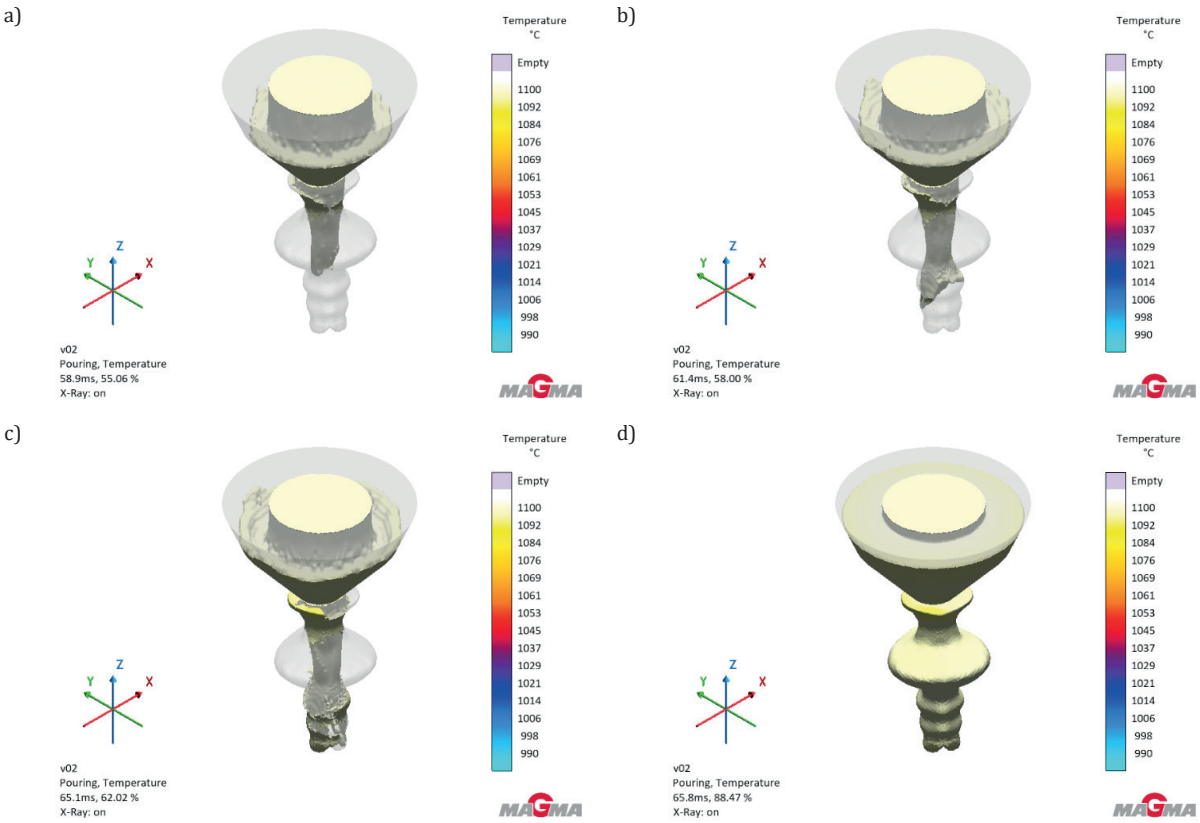

Fig. 4. Pouring simulation results in MAGMASOFT® 6.1 for the 3D scanned model at four stages of mould cavity filling: a) 55.06%; b) 58.00%; c) 62.02%; d) 88.47%

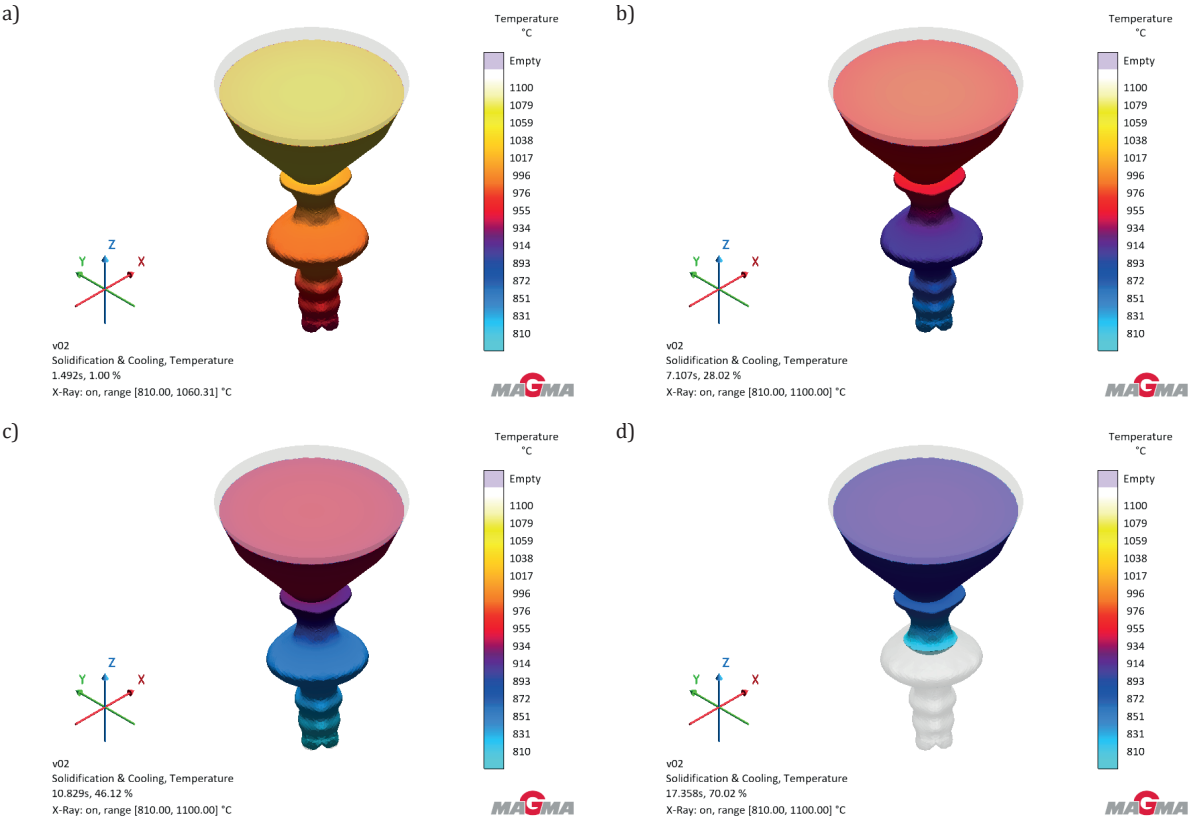

Fig. 5. Solidification simulation results in MAGMASOFT® 6.1 for the scanned model at four stages of mould cavity solidification: a) 1.00%; b) 28.02%; c) 46.12%; d) 70.02%

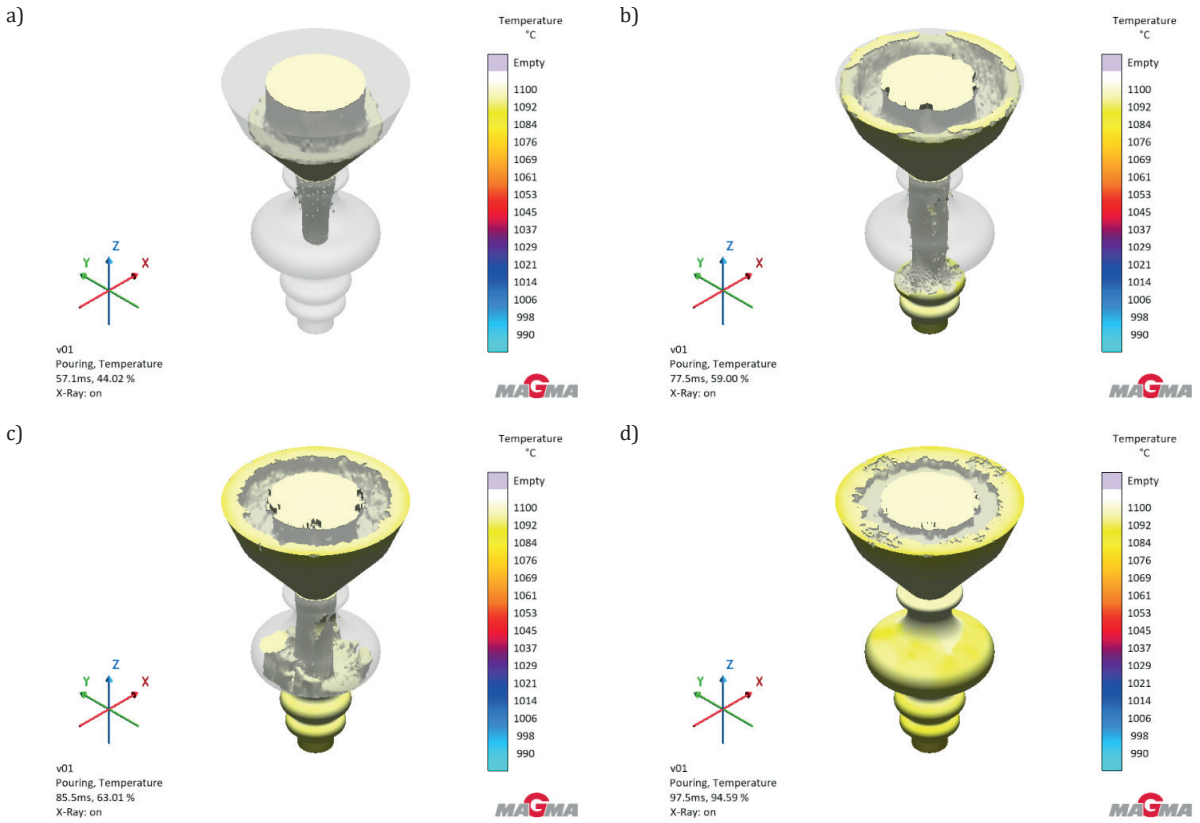

Fig. 6. Pouring simulation results in MAGMASOFT® 6.1 for the 3D CAD model at four stages of mould cavity filling: a) 44.02%; b) 59.00%; c) 63.01%; d) 94.59%

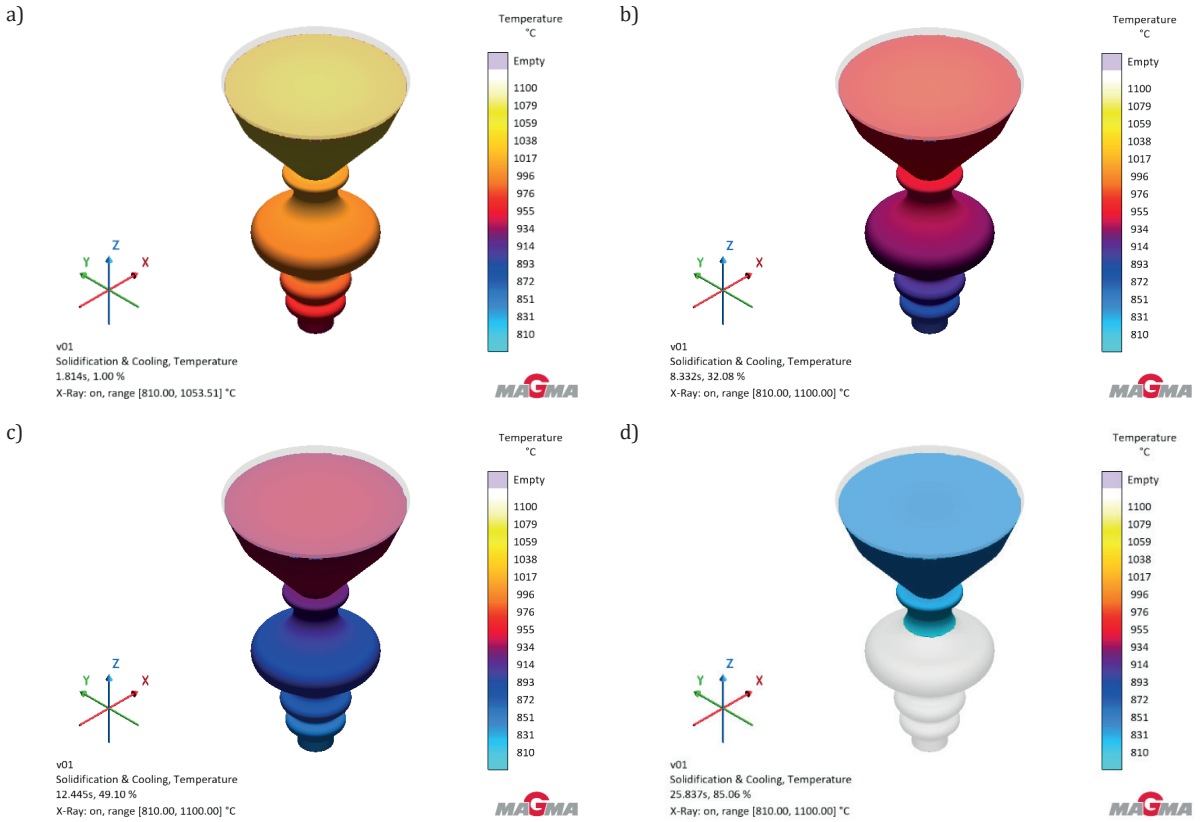

Fig. 7. Solidification simulation results in MAGMASOFT® 6.1 for the 3D CAD model at four stages of solidification process: a) 1.00%; b) 32.08%; c) 49.10%; d) 85.06%

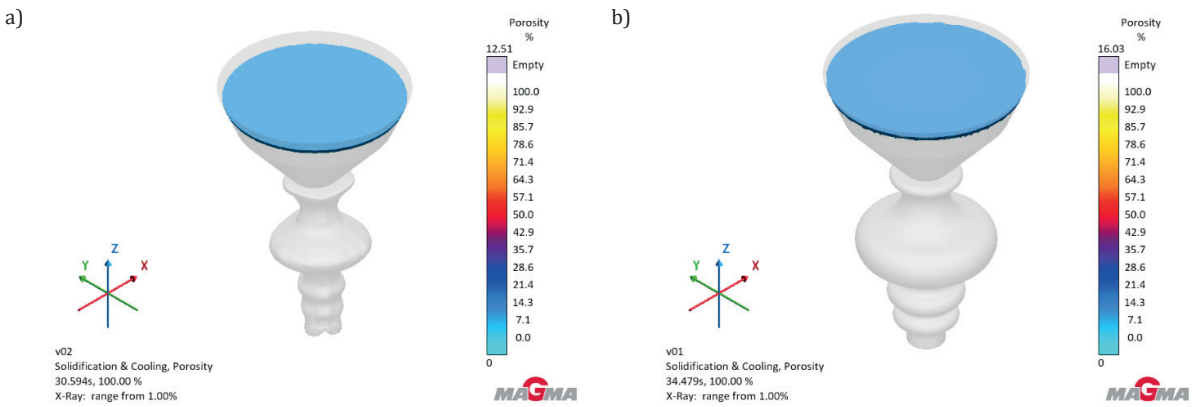

Fig. 8. Comparison of predicted porosity results in MAGMASOFT® 6.1 for the 3D scanned model (a) and the 3D CAD model (b)

The results of casting the modern replica of the object provided valuable comparative material, enabling the correlation of the numerical simulation predictions with the real behaviour of the copper alloy inside the ceramic mould. The model intended for casting, previously prepared in SOLIDWORKS 2023, was reproduced using 3D printing with photopolymer resin. The model obtained exhibited a smooth surface and high precision in detail reproduction, which was crucial for subsequent comparison with the original object and for reconstructing the thin-walled segments visible in the 3D scan.

The mould was prepared using a refractory mass, which, after initial setting, was subjected to resin burnout and ceramic shell heating, following a temperature schedule recommended by the manufacturer. After reaching the target temperature, the mould obtained the thermal and mechanical stability required to receive the molten metal.

The casting was produced using the centrifugal method with a casting centrifuge, which enabled rapid and uniform introduction of the CuSn12 copper alloy into the thin and complex regions of the mould cavity. During pouring, the alloy was introduced into the mould at a temperature close to that used in the simulations, ensuring the possibility of directly comparing the actual process course with the computational model. After cooling, the ceramic shell was removed, and the raw casting was mechanically cleaned.

The obtained casting, presented in Figure 9, exhibits characteristic surface features of castings produced using the investment casting method, including subtle differences resulting from the quality of the ceramic mass and the spinning parameters. The casting retained key geometrical features, enabling assessment of the consistency between the reconstruction model and the real metallurgical process. The thin-walled regions were reproduced without deformation, confirming that both the mould preparation and the metal flow dynamics in the centrifuge were consistent with the simulation predictions.

3D printing of the CAD model enabled comparison of geometric behaviour in an additive manufacturing process. The print obtained on the AL3D printer is presented in Figure 10. The model was faithfully reproduced, including the thin-walled segments, confirming the accuracy of the reconstruction and demonstrating the usefulness of 3D printing as an additional tool for assessing the geometry of the artefact. The printed model made it possible to analyse the proportions of the original form in physical space.

Fig. 9. Casting obtained using the investment casting method

Fig. 10. Object produced using a 3D printer

The obtained reconstruction enabled a comparison with the cast replica and the original object. Comparative analysis

of these three forms, the classical casting, the additively manufactured reconstruction, and the 3D scan data, allowed the identification of differences resulting from the manufacturing technologies and confirmed the usefulness of both techniques for reconstructing archaeometallurgical objects [22–24].

4. CONCLUSIONS

The conducted research confirmed that the use of integrated reconstruction methods, including 3D scanning, CAD-based modelling, casting simulations, 3D metal printing, and investment casting, allows for a comprehensive recreation of both the geometry and the potential manufacturing process of the analysed object. The obtained digital models demonstrated consistency with the predicted filling and solidification conditions, while the physical reconstructions further validated the technological assumptions. At the same time, the material characteristics of the artefact can be considered typical for castings of a similar origin, which situates it within the context of known metallurgical practices.

These studies highlight the importance of an interdisciplinary approach, where reverse engineering, digital tools, foundry techniques, and additive manufacturing technologies complement each other, creating a coherent reconstruction model. The results obtained represent one stage of a longer research process conducted at the Historical Layers Research Centre AGH, where the object was analysed and where the subsequent stages of the project are being carried out. Further work is planned, including additional comparisons of reconstructions, an expanded analysis of simulation parameters, and testing of alternative technological variants. This will enable an even more complete reconstruction of the object's production process and a better understanding of the relationships between its geometry, material, and historical casting technique.

ACKNOWLEDGMENTS

The work was funded under the European Funds for a Modern Economy 2021–2027 programme FENG 2.4 Badawcza Infrastruktura Nowoczesnej Gospodarki FENG.02.04-IP.04-001/24 MAPA pt. Polska infrastruktura dla badań nad dziedzictwem kulturowym – ERIHS.PL, conducted at the AGH University of Science and Technology. The provided funding enabled the use of modern, interdisciplinary methods of analysis and reconstruction, which were essential for the comprehensive elaboration of the results presented in this article.

REFERENCES

[1] Garbacz-Klempka A., Rosołowski S., Gackowski J., Wardas-Lasoń M., Dąbrowski H. P., Fijołek A., Piękoś M., Kozana J., Tabaszewski W., Jurecki P., Wałach D., Kaczmarczyk G. & Marlicka K. (2024). Wytwórczość brązownicza w grodzie kultury łużyckiej w Biskupinie w świetle wyników badań archeometalurgicznych. In: *90. rocznica rozpoczęcia badań wykopaliskowych w Biskupinie: jubileuszowa Konferencja Naukowa: 7–8 listopada 2024.* Biskupin: Muzeum Archeologiczne.

[2] Fijołek A., Garbacz-Klempka A., Wardas-Lasoń M., Marlicka K., Piekło J., Piękoś M., Kozana J. & Wałach D. (2025). Archaeometallurgy using modern research techniques and reverse engineering. Results obtained and prospects for the future. In: *ICME 25: V International Conference of Casting and Materials Engineering: Lightweight Innovations for a Better Climate: Krakow, Poland, October 27–28, 2025*. Krakow: AGH University of Krakow, Faculty of Foundry Engineering.

[3] Garbacz-Klempka A., Suchy J. S., Kwak Z., Długosz P. & Stolarczyk T. (2018). Casting technology experiment and computer modeling of ornaments from Bronze Age. *Archives of Metallurgy and Materials*, 63(3), 1329–1337. DOI: https://doi.org/10.24425/123808.

[4] Garbacz-Klempka A., Piękoś M., Perek-Nowak M., Kozana J., Żak P., Fijołek A., Silska P. & Stróżyk M. (2022). Reconstruction of the Late Bronze Age foundry process in Greater Poland: Analyses and simulations. Case study of hoard from Przybysław. *Archives of Metallurgy and Materials*, 67(3), 1125–1136. DOI: https://doi.org/10.24425/amm.2022.139712.

[5] Garbacz-Klempka A., Kwak Z., Żak P. L., Szucki M., Ścibior D., Stolarczyk T. & Nowak K. (2017). Reconstruction of the casting technology in the Bronze Age on the basis of investigations and visualisation of casting moulds. *Archives of Foundry Engineering*, 17(3), 184–190. DOI: https://doi.org/10.1515/afe-2017-0113.

[6] Garbacz-Klempka A., Rzadkosz S., Stolarczyk T., Piękoś M. & Kozana J. (2013). Archaeological remains of the copper metallurgy in Lower Silesia. *Metallurgy and Foundry Engineering*, 39(2), 29–36. DOI: https://doi.org/10.7494/mafe.2013.39.2.29.

[7] Liu B., Zhang F., Sun X. & Rushworth A. (2023). Additive manufacturing in cultural heritage preservation and product design. In: Pei E., Bernard A., Gu D., Klahn Ch., Monzón M., Petersen M., Sun T. (Eds.), *Springer Handbook of Additive Manufacturing*. Cham: Springer International Publishing, pp. 923–940.

[8] Cleary P., Ha J., Alguine V. & Nguyen T. (2002). Flow modelling in casting processes. *Applied Mathematical Modelling*, 26(2), 171–190. DOI: https://doi.org/10.1016/S0307-904X(01)00054-3.

[9] Prochaska M. & Mitka B. (2016). RevoScan – automatic device for 3D digitisation: Concept, application, test results. *Geomatics and Environmental Engineering*, 10(4), 81–87. DOI: https://doi.org/10.7494/geom.2016.10.4.81.

[10] Davey C.J. (2009). The early history of lost-wax casting. In: Mei J., Rehren T. (Eds.), *Metallurgy and Civilisation: Eurasia and Beyond*. London: Archetype Publications, pp. 147–154.

[11] Hunt B.L. (1980). The long history of lost wax casting: Over five thousand years of art and craftsmanship. *Gold Bulletin*, 13(2), 63–79. DOI: https://doi.org/10.1007/BF03215456.

[12] Kantaros A., Ganetsos T. & Petrescu F.I.T. (2023). Three-dimensional printing and 3D scanning: Emerging technologies exhibiting high potential in the field of cultural heritage. *Applied Sciences*, 13(8), 4777. DOI: https://doi.org/10.3390/app13084777.

[13] Bašić A., Mladineo M., Peko I. & Aljinović Meštrović A. (2018). 3D scanning, CAD optimization and 3D print application in cultural heritage: An example on statue from the ancient Salona. In: *8th International Conference "Mechanical Technologies and Structural Materials 2018", Split, Croatia, 27–28 September 2018*.

[14] Balletti C., Ballarin M. & Guerra F. (2017). 3D printing: State of the art and future perspectives. *Journal of Cultural Heritage*, 26, 172–182. DOI: https://doi.org/10.1016/j.culher.2017.02.010.

[15] Elias C. (2019). Whose digital heritage? Contemporary art, 3D printing and the limits of cultural property. *Third Text*, 33(6), 687–707. DOI: https://doi.org/10.1080/09528822.2019.1667629.

[16] Parfenov V., Igoshin S., Masaylo D., Orlov A. & Kuliashou D. (2022). Use of 3D laser scanning and additive technologies for reconstruction of damaged and destroyed cultural heritage objects. *Quantum Beam Science*, 6(1), 11. DOI: https://doi.org/10.3390/qubs6010011.

[17] Duda T. & Raghavan L. V. (2016). 3D metal printing technology. *IFAC-PapersOnLine*, 49(29), 103–110. DOI: https://doi.org/10.1016/j.ifacol.2016.11.111.

[18] Sadiq Al-Baghdadi M.A.R. (2017). 3D printing and 3D scanning of our ancient history: Preservation and protection of our cultural heritage and identity. *International Journal of Energy and Environment*, 8(5), 441–456.

[19] Nancharaiah T. (2020). A review paper on metal 3D printing technology. In: Patnaik A., Kozeschnik E., Kukshal V. (Eds.), *Advances in Materials Processing and Manufacturing Applications. Proceedings of iCADMA 2020*, Springer, pp. 251–259. DOI: https://doi.org/10.1007/978-981-16-0909-1_25.

[20] Konda Gokuldoss P., Kolla S. & Eckert J. (2017). Additive manufacturing processes: Selective laser melting, electron beam melting and binder jetting – Selection guidelines. *Materials*, 10(6), 672. DOI: https://doi.org/10.3390/ma10060672.

[21] Sefene E.M. (2022). State-of-the-art of selective laser melting process: A comprehensive review. *Journal of Manufacturing Systems*, 63, 250–274. DOI: https://doi.org/10.1016/j.jmsy.2022.04.002.

[22] Scudino S., Unterdörfer C., Prashanth K.G., Attar H., Ellendt N., Uhlenwinkel V. & Eckert J. (2015). Additive manufacturing of Cu–10Sn bronze. *Materials Letters*, 156, 202–204. DOI: https://doi.org/10.1016/j.matlet.2015.05.076.

[23] Padovezzi R.O., Garcia Trindade W., Marques G.A., Pereira Gomes Pinto E., Costa Silva M., Amorese R.A., Santos Damasio T. & Tedardi do Nascimento P.H. (2025). Effects of the additive manufacturing process on the mechanical and structural properties of bronze alloys: A review. *Revista de Gestão e Secretariado*, 16(7), 5057–5057. DOI: https://doi.org/10.7769/gesec.v16i7.5057.

[24] Rahmani R., Resende P.R., Couto R., Lopes S.I., Kumar R., Maurya H.S., Karimi J, Afonso A.M., Hussain A. & Abrantes J.C.C (2024). Structural analysis of selective laser melted copper-tin alloy. *Journal of Alloys and Metallurgical Systems*, 7, 100097. DOI: https://doi.org/10.1016/j.jalmes.2024.100097.